Astron. Astrophys. 333, 43–47 (1998)

ASTRONOMY AND ASTROPHYSICS

Imaging around PC 1643+4631A at the Lyman limit

I. Ferreras[1,2], **N. Benítez**[1,2], **and E. Martínez-González**[1]

[1] Instituto de Física de Cantabria, CSIC-Universidad de Cantabria, Fac. de Ciencias, Av. los Castros s/n, E-39005 Santander, Spain (ferreras@ifca.unican.es)
[2] Departamento de Física Moderna, Universidad de Cantabria

Received 12 December 1997 / Accepted 15 January 1998

Abstract. We present a list of candidates for high redshift late–type galaxies in the field around the $z = 3.79$ quasar PC 1643+4631A. Deep U,V and R imaging has been used to search for objects with a strong Lyman break between U and V, characteristic of galaxies with high hydrogen column densities at $z \sim 3$. A further study of the red objects detected by Hu & Ridgway (1994) has been done, allowing the tentative identification of many of them as low redshift ($z \sim 0.4$) elliptical galaxies.

Key words: cosmology: observations – galaxies: formation – galaxies: distances and redshifts – quasars: individual: PC 1643+4631A

1. Introduction

One of the most efficient methods of selecting high redshift galaxy candidates involves the detection of Lyman break systems. This break comes from the likelihood of absorption due to intervening H I along the line of sight and — for many galaxies — also from the instrinsic continuum break in the spectrum of the galaxy (Bruzual & Charlot 1993). The search is done with two broad band filters that fork this break and a third one that is used to further ascertain the high redshift nature of the object. The work of Steidel et al. (1992, 1993,1995) imaging fields around high redshift quasars yielded many candidates, several of which have been spectroscopically confirmed to be galaxies at $z \approx 3$. The advantage over previous unsuccessful narrowband Lyman-α surveys (e.g. Giavalisco et al. 1994, Martínez-González et al. 1995) is that a wide range in redshift can be surveyed. Besides, the break in the spectrum can be easily discerned with broad band imaging, allowing the detection of normal high-z galaxies, with a typical magnitude at a redshift of $z \sim 3$–4 of $R \sim 25^m$ (Djorgovski 1997). Furthermore, the Lyman-α emission line can be weak or even non-existent as it appeared in many of the galaxies detected by Steidel et al. 1996.

We found the field around quasar PC 1643+4631A to be a good candidate for this technique for a couple of reasons: This $z = 3.79$ QSO has a Damped Lyman-α System (DLS) at $z = 3.14$ (Schneider et al. 1991) whose Lyman break would be perfectly positioned between Johnson U and V filters. Besides, a possible very massive cluster might exist between this quasar and a second one (PC 1643+4631B) that lies just 200 arcsec away and has roughly the same redshift ($z = 3.831$). Jones et al. 1997 detected a significant decrement in the CMB in a region between these two QSOs that could be related with a Sunyaev-Zeldovich effect arising from a M$\sim 10^{15}$M$_\odot$ intervening cluster. However, Saunders et al. 1997 imaged the region in R,J and K bands, looking for ellipticals that should abound in such a cluster, and found no evidence. The technique used in this paper is the best one to search for galaxies in the redshift range $z \sim 3 - 4$, thereby contributing to check this result: If such a massive cluster were to exist, a survey around PC 1643+4631A should give a net excess of candidates towards the direction of the cluster.

Send offprint requests to: I. Ferreras

Table 1. Imaging around PC 1643+4631A

Band	Exposure Time (sec.)	Seeing	Lim. Mag.
U	18000 (NOT) + 2400 (WHT)	$1.2''$	26.0
V	3600 (WHT)	$1.0''$	26.0
R	7200 (NOT) + 1800 (WHT)	$1.5''$	26.0

2. Observations

The observations were obtained in May 1996 using BroCam2 at the 2.5 m Nordic Optical Telescope (NOT) and in May 1997 using the William Herschel Telescope (WHT) 4.2 m prime focus camera, both at the Roque de los Muchachos Observatory, La Palma, Spain. Both cameras used a thinned 2048×2048 Loral chip which is remarkable for its very high quantum efficiency even in the blue part of the spectrum, making it especially useful for U band imaging. The image scale is $0.11''$ and $0.265''$ per pixel (NOT and WHT respectively). We also used a 30 minute exposure of the quasar in the R band (WHT+TEK CCD detector) taken by Saunders....., retrieved from the ING archive, which greatly helped us in achieving a homogenous limiting magnitude in all three bands. Deep imaging was done through Johnson U, V and R filters and reduced using the standard techniques of bias subtraction and flat fielding using IRAF tasks. The long integration times required were separated into shorter — usually 1200 second — exposures, slightly nodding the tele-

Table 2. Lyman Break Candidates within 1.5 arcmin

No.	$\Delta\alpha('')$	$\Delta\delta('')$	V	$U-V$	$V-R$
1	-0.3	-6.6	24.09	0.97	0.78
2	-5.6	7.4	25.00	>1.00	-0.16
3	-22.2	10.8	24.64	>1.36	-0.11
4	8.4	-29.9	24.57	0.77	-0.24
5	-27.0	29.0	25.22	>0.78	-0.27
6	-21.3	-34.2	24.57	>1.43	0.12
7	1.4	42.6	25.36	>0.64	0.43
8	63.2	-0.7	24.96	0.70	0.14
9	9.9	-43.5	25.30	>0.70	0.14
10	-64.9	-3.2	24.09	0.90	-0.01
11	59.1	-29.4	24.52	>1.48	-0.18
12	31.4	-46.9	24.67	>1.33	0.46
13	8.4	-54.5	24.79	>1.21	-0.00
14	28.2	-57.0	24.30	0.77	-0.21
15	58.6	49.0	24.98	>1.02	0.09
16	-66.1	-44.5	25.24	>0.76	0.01
17	79.3	33.2	25.23	>0.77	0.81
18	-23.7	71.3	24.72	>1.28	-0.20
19	-12.4	74.0	24.24	0.92	0.22
20	-82.7	-55.3	25.43	>0.57	-0.17
21	-18.9	82.5	24.80	0.45	0.67

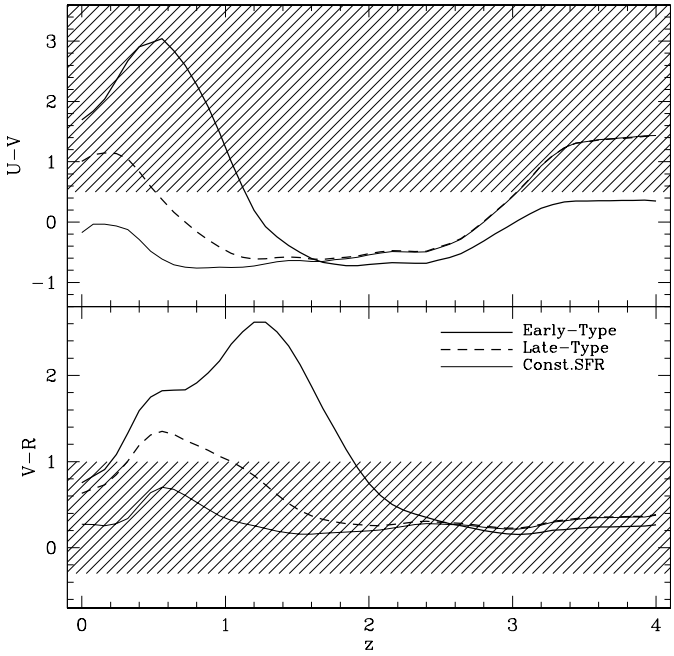

Fig. 1. Predictions for three different morphologies from the spectral evolution models of Bruzual & Charlot (1997). The shaded areas represent the color constraints when choosing candidates for high-redshift galaxies.

scope between them in order to be able to eliminate cosmic rays and bad pixels. These frames were eventually registered and combined into a final image using a clipping algorithm. The photometric calibration was achieved with images of standard stars (Landolt 1992) taken throughout the observing nights.

In order to detect candidates of galaxies at high redshift, a very deep exposure must be achieved in each filter. The deepest band should be U because it represents the spectral range shortward of the Lyman break for $z \approx 3$ objects.

3. Analysis

The search of objects in the final frames was performed using SExtractor (Bertin E. 1996), carefully tweaking the parameters to avoid such effects as excessive deblending or noise–dominated detections. The threshold was set at 16 connected pixels (which is slightly smaller than the number of pixels inside the seeing disk) with 0.75σ lower limit per pixel for a global 3σ detection per object. We performed aperture photometry on the objects using several aperture sizes to make sure we were collecting all the flux. It also gave us an idea of the uncertainty to expect with faint objects. Finally, we chose a diameter of 12 pixels (3.2 arcsec) to get the photometry and checked each candidate visually to make sure there was no problem with deblending, hot pixels or other spurious detections. This issue was further enforced by considering only candidates that appeared both in the V and R filter images. The size of the aperture was chosen taking into account the seeing of the images (1–1.5 arcsec) and the fact that high–z candidates should be pointlike objects.

The photometry output from SExtractor was further checked using several tasks from IRAF from which we can extract a photometric uncertainty of 0.3–0.4 magnitudes for objects with $V > 24^m$. The candidates for high redshift galaxies were obtained using a color and magnitude constraint. The first and most important one is $U - V > 0.5$ since it reveals the existence of a break in the spectrum at around 3650Å which corresponds to the Lyman continuum break at $z \sim 3$. Unfortunately, there is also a very strong break at 4000Å in the rest frame, especially prominent in old galaxies. Hence, low-z early–types can sneak in our list. Furthermore, we could also find galaxies with a strong emission line falling in the V band and faking such a break. The way out of this degeneracy is twofold: we check an extra color towards the red side of the spectrum, namely $V - R$, which can tell low redshift ellipticals or galaxies with strong emission lines from high redshift ones. We took $-0.3 \leq V - R \leq 1.0$. Fig. 1 shows the color prediction for three different morphologies from the models of Bruzual & Charlot 1997. Notice how the degeneracy between high redshift late–type galaxies and low redshift ellipticals in the $U - V$ graph is removed when considering $V - R$.

An early–type galaxy has a steeper spectrum towards R, thereby higher values of $V - R$, whereas the lower bound in this color is chosen to avoid galaxies with strong emission lines which might fall in the V band. Besides the color constraints, we should also impose a limit on the apparent magnitude. Even though the selection suffers from Malmquist's bias, we do not expect to find galaxies with an intrinsic luminosity greater than a few $L_\star$, which implies rejecting candidates whose apparent magnitude is brighter than $V \sim 24^m$. Part of the degeneracy may still remain because faint galaxies could still be identified with ellipticals at low redshift with an absolute luminosity

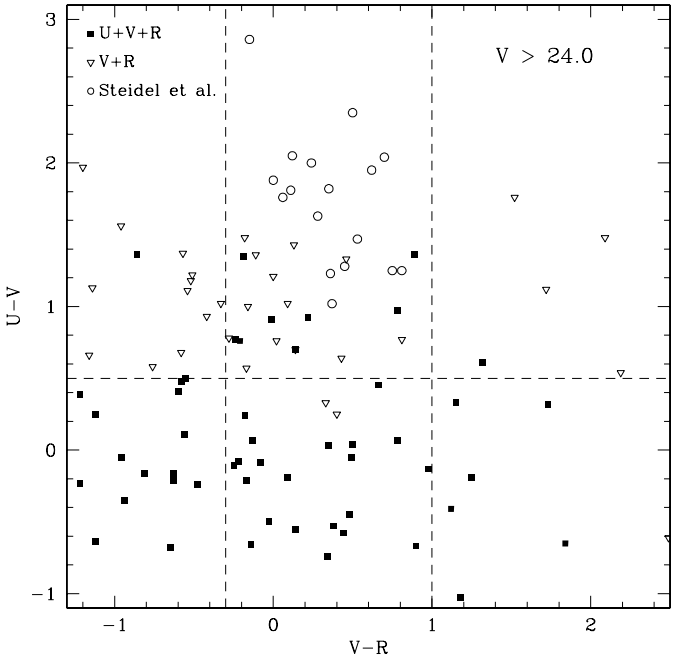

Fig. 2. Color–Color diagram of faint ($V > 24^m$) objects detected around PC 1643+4631A. The dashed lines engulf the region inside which proper candidates must lie. These objects use different symbols depending on whether there has been a matching detection in the R or U band (as well as the V band which is used as reference). The confirmed $z \approx 3$ galaxies listed in Steidel et al. (1996) are also shown.

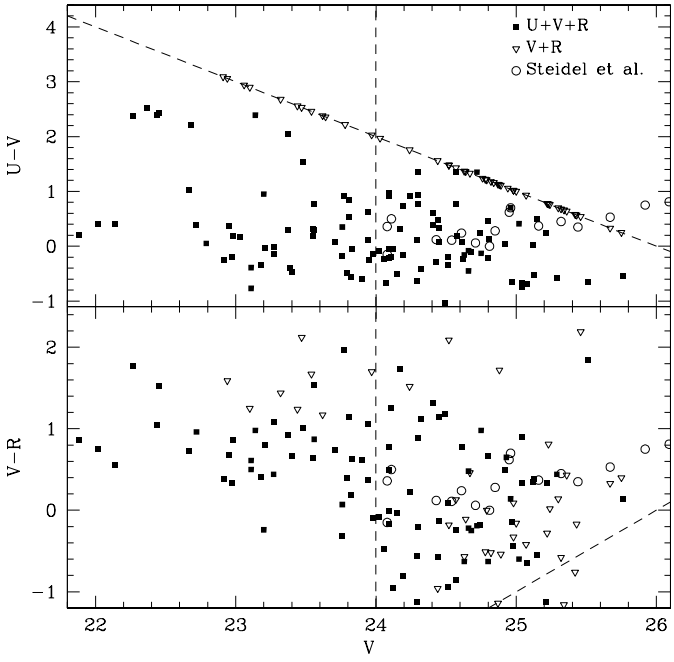

Fig. 3. Color–Magnitude diagrams for objects around PC 1643+4631A detected both in V and R. The dashed lines represent the limiting magnitude. Steidel et al.'s confirmed candidates are also shown.

around $L < 0.04L_\star$. However, the constraint in $V - R$ makes this choice less likely over a late–type high redshift galaxy.

Table 2 shows the list of candidates which appeared in our images imposing these constraints. All the objects with detections both in V and R are shown in Fig. 3, whereas Fig. 2 plots a subsample of these objects with $V > 24.0^m$ and shows the constraining color–color region where the candidates should lie. Fig. 2 also shows the confirmed candidates from Steidel et al. (1996), who used the same technique although with a different set of filters, specifically designed for maximum efficiency at these redshifts.

Finally, we considered the object that lies very close to the line of sight of the QSO. The V and R images show it as an elongation of the quasar towards the SW, but in the U band it stands out clearly as the QSO fades out of view. In order to perform the photometry in V and R, we subtracted the PSF of a nearby point-like object scaled to the peak of the QSO. This is just a rough estimate but it allows us to ascertain the nature of this object. We got $V = 22.7$; $U - V = 0.3$ and $V - R = 1.6$. It is rather bright in the U band, which discards the possibility of it being the one responsible for the DLS in the QSO's spectrum at $z = 3.14$. The models fit these colors with a late–type galaxy at $z \sim 0.5$, which — for a $\Omega_0 = 1$, $h_0 = 0.5$ cosmology — gives an absolute luminosity of $L \sim 0.2L_\star$. This galaxy might possibly leave its imprint on the spectrum of the QSO.

4. Hu & Ridgway's red objects revisited

Among the many objects detected around PC 1643+4631A, it is worth mentioning a group of them that are very red in $U - V$ but too bright to be high redshift galaxies. Many of these objects were already detected by Hu & Ridgway (1994), using a selection criteria in the red and NIR part of the spectrum. They looked for objects which had a very red $I - K$ color, hence aiming at the detection of early–type galaxies and EROS. The 19 objects listed in their work are shown in Table 3 along with our photometry in U,V and R. Combining both surveys we have photometry in 8 standard filters (U, B, V, R, I, J, H, K') which can be used to determine the nature of some of these objects. Most of them have very red $U - V$ and $R - K'$ colors as well as relatively bright V magnitudes, all evidence pointing at low redshift elliptical galaxies. The high density of these objects may plausibly imply the existence of a cluster. Furthermore, radio–loud QSOs — such as PC 1643+4631A — have a higher probability of being magnified by foreground matter (i.e. an intervening cluster) because of the double magnification bias (Benítez & Martínez-González 1995, Schneider et al. 1997). The last entry in Table 3 gives an estimated redshift using the models of Bruzual & Charlot (1997). The square difference between the actual and the predicted models is computed and the z for which this difference reaches a minimum gives the estimated redshift. The letter in front labels the type of galaxy model that fits best: E and L for early and late type, respectively.

Objects # 10 and 14 cannot be catalogued this way because they escape detection down to very faint magnitudes ($U > 26^m$ and $V > 26^m$). They are very good candidates for EROS and that prompted the observations of object # 10 doing deep IR

Table 3. Red Objects from Hu & Ridgway 1994. The quasar is object # 7.

No.	V	$U-B$	$B-V$	$V-R$	$R-K'$	$z_{\rm FIT}$
1	20.8	1.4	1.3	2.4	2.7	E/0.5
2	19.3	1.3	1.2	1.2	2.2	E/0.4
3	20.2	-0.6	1.9	1.0	3.1	—
4	19.8	-1.1	1.7	0.7	2.6	—
5	20.6	1.4	1.3	1.5	2.5	E/0.4
6	21.4	0.0	1.5	1.5	2.7	L/0.4
7	20.2	>4.6	1.2	0.7	2.2	—
8	21.8	>2.7	1.0	0.9	2.9	E/0.4
9	23.8	-0.6	1.6	2.0	3.6	E/1.0
10	>26.0	>-1.0	<0.5	—	>6.6	—
11	23.0	>0.7	1.8	2.0	2.6	E/0.4
12	24.1	-0.8	0.7	1.3	4.4	—
13	24.0	>0.3	1.2	1.9	3.6	E/0.4
14	>26.0	—	—	—	>6.3	—
15	21.4	-1.0	1.3	0.1	2.5	—
16	23.0	-1.2	0.9	0.4	3.7	—
17	23.4	>0.2	1.9	1.5	3.0	E/0.3
18	22.7	0.0	1.7	0.3	3.5	—
19	22.4	>1.9	1.2	0.9	2.5	E/0.4

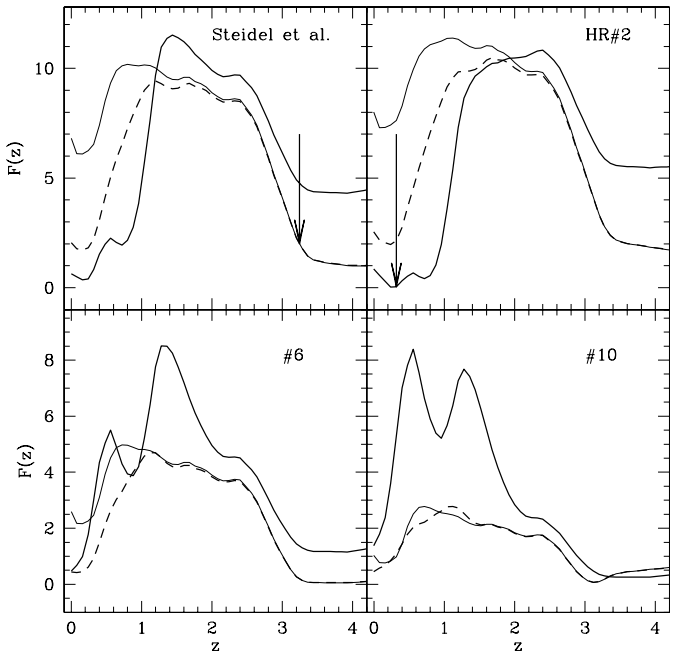

Fig. 4. Color–color fit to spectra from the models of Bruzual & Charlot (1997) for (clockwise from upper left) one of Steidel et al's (1996) confirmed high-z galaxies, one of Hu & Ridgway's (1994) red object, and a couple of our candidates. F(z) represents the sum of the squares of the differences in $U-V$ and $V-R$ between the actual colors and the ones from the models. The thick,dashed and thin lines represent early–type, late–type and constant SFR, respectively. The arrow in Steidel et al.'s box show the actual redshift of the object, the one in Hu & Ridgway's box show the expected low redshift value which is also considered against high-z from the bright nature ($V=19.3$) of the object.

imaging and spectroscopy (Graham & Dey 1996), finding — as expected — that it could not be an elliptical galaxy but rather an interacting system. A possible Hα emission at $z\approx 1.44$ was detected, revealing quite a strong star formation rate.

5. Conclusions

The search for the Lyman break in high redshift galaxies is so far the most efficient way of selecting candidates for follow-up spectroscopy. The field around PC 1643+4631A ($z=3.79$) is a very attractive target for this method since it has a DLS at $z=3.14$ which sets the Lyman break between Johnson U and V frames. We performed deep imaging in U,V and R and obtained a list of candidates for late–type high redshift galaxies. The claim of Jones et al. (1997) that a massive cluster might lie close to this QSO — based on a Sunyaev-Zeldovich detection — cannot be confirmed as the listed candidates are distributed homogeneously over the frame. Our result corroborates the work of Saunders et al. (1997), who did not detect any overabundance of objects in NIR images (aiming at the detection of early–type galaxies).

Besides, this work has completed the data from Hu & Ridgway (1994) for a sample of 18 objects around the quasar which have a very red $I-K$ color. The addition of U, V and R photometry to these objects allows a better identification. We found many of them to match the colors for early–type normal galaxies at $z\sim 0.4$. The extremely red objects # 10 and 14 in the list from Hu & Ridgway's work are fainter than the limiting magnitude of our search ($U,V,R>26.0$) which means these two objects must have a very steep rise towards the NIR part of the spectrum.

Acknowledgements. The WHT and NOT are operated on the island of La Palma by the Royal Greenwich Observatory and the Nordic Optical Telescope Scientific Association, respectively, in the Spanish Observatorio del Roque de los Muchachos of the Instituto de Astrofísica de Canarias. We would like to thank the Isaac Newton Group of Telescopes for such a friendly interface to retrieve images from its archive. I.F. and N.B. acknowledge a Ph.D. scholarship from the 'Gobierno de Cantabria', and the Spanish MEC, respectively. I.F.,N.B. and E.M.-G. acknowledge financial support from the Spanish DGES under contract PB95-0041.

References

Benítez N., Martínez-González E., 1995 ApJL 448, L89.
Bertin E., Arnouts S., 1996 A& AS 117, 393.
Bruzual A. G., Charlot S., 1993 Ap.J. 405, 538
Bruzual A. G., Charlot S., 1997 In preparation
Giavalisco M., Macchetto F. D., Sparks W. B., 1994 A& A 288, 103
Graham J. R., Dey A., 1996 Ap.J. 471, 720
Hu E. M., Ridgway S. E., 1994 A.J. 107, 1303
Djorgovski S. G., 1997 astro-ph 9709001
Jones M. E., Saunders R., Baker J. C., Cotter G., Edge A., Grainge K., Haynes T., Lasenby A., Pooley G., Röttgering H., 1997 Ap.J.Lett. 479, 1
Lacy M., Rawlings S., 1996 MNRAS 280, 888
Landolt A. U., 1992 A.J. 104, 340

Martínez-González E., González-Serrano J. I., Cayón L., Sanz J. L., Martín-Mirones J. M., 1995 A& A 303, 379
Saunders R., Baker J. C., Bremer M. N. et al., 1997 Ap.J.Lett. 479, 5
Schneider D. P., Schmidt M., Gunn J. E., 1991 A.J. 101, 2004
Schneider P. et al. 1997 astro-ph/9705122.
Steidel C. C., Hamilton D., 1992 A.J. 104, 941
Steidel C. C., Hamilton D., 1993 A.J. 105, 2017
Steidel C. C., Pettini M., Hamilton D., 1995 A.J. 110, 2519
Steidel C. C., Giavalisco M., Pettini M., Dickinson M., Adelberger K. L., 1996 Ap.J.Lett. 462, 17